

# Comparison of Landsat and ASTER in Land Cover Change Detection within Granite Quarries

R. S. Moeletsi<sup>1,2</sup> and S. G. Tesfamichael<sup>1</sup>

<sup>1</sup>Department of Geography, Environmental Management and Energy Studies,  
University of Johannesburg, Auckland Park, 2006, Johannesburg, South Africa

<sup>2</sup>Mintek, 200 Malibongwe Drive, Randburg, 2125, South Africa

Keywords: Granite Quarries, Landsat, ASTER, Accuracy Assessment.

Abstract: This study evaluated and compared the utility of Landsat and ASTER in land cover change detection within granite quarries. Landsat data used was acquired in 1998 and 2015 while ASTER data used was acquired in 2001 and 2013. Both Landsat and ASTER were classified using supervised and maximum likelihood classification. Post-classification and Normalized Difference Vegetation Index change detection techniques were applied to assess and measure changes in land cover caused by granite quarries. Overall classification of ASTER was slightly higher than that obtained for Landsat (overall accuracy (OA) =79% and kappa 0.75 vs. OA=75% and kappa 0.71). Both Landsat and ASTER were able to assess land cover changes within granite quarries. Change detection results revealed increase in granite quarries which subsequently resulted in decrease in vegetation and bare land and increase in water bodies within the quarries. The study found ASTER to be better at discriminating granite quarries from other land cover features and was able to detect small water bodies within granite quarries due to higher spatial resolution of bands in the VNIR subsystem. On the contrary, Landsat was found better at detecting changes in vegetation within granite quarries.

## 1 INTRODUCTION

Remote sensing techniques are useful in mapping, monitoring and managing land cover changes related to mining activities (López-Pamo *et al.*, 1999). Coupled with capabilities to cover large areas, availability of historic data, availability of data at high spatial and spectral resolution, the technology is continuously contributing significantly to land management initiatives (Rogan and Chen, 2004). Several studies have used remotely sensed data ranging from low to high spatial resolution sensors such as MODIS, NOAA AVHRR, Landsat, ASTER, SPOT, and IKONOS in change detection studies (Lu *et al.*, 2004). Even though the use of remotely sensed data has been widely utilized in land use and land cover change (LULCC), its applications in mapping impacts of surface mining have not been extensively explored (Latifovic, 2005). This paper therefore compares utility of Landsat and ASTER satellite sensors in land cover changes caused by granite quarries located in the North West province of South Africa.

Mining is an integral part of economic development in many developing countries, however, it is

often associated with adverse environmental and social impacts (Paull *et al.*, 2006). Granite quarrying in South Africa started in the late 1930s in Bon-Accord area. Quarrying adversely affects environment in various ways. Common environmental impacts resulting from quarrying activities include loss of vegetation, disruption and destruction of natural habitat (Maponga and Munyanduri, 2001), and can alter hydrological systems (Darwish *et al.*, 2011). It is therefore important to monitor environmental variables related to mining activities. Identifying and monitoring such impacts contributes to sustainable development and provides information regarding rehabilitation measures, future site selection methods and determining locations of abandoned and unreclaimed quarries (Demirel *et al.*, 2011).

## 2 STUDY AREA

Granite quarrying in South Africa occurs in the Main Zone of the Rustenburg Layered Suite in the Bushveld Igneous Complex. The area is dominated

by gabbro and norite with interlayered anorthosite of the pyramid Gabbro-Norite, Rustenburg Layered Suite (Nex *et al.*, 1998). The quarries are located between Rustenburg and Brits towns in the North West Province (Figure 1). Commercially, the word granite refers to any crystalline rock exploited for use in the construction and ornamental use (Dolley, 2007). Granite mining in the North West province contributed 46 of the national mining of granite in 2008 (Lamprecht *et al.*, 2011).

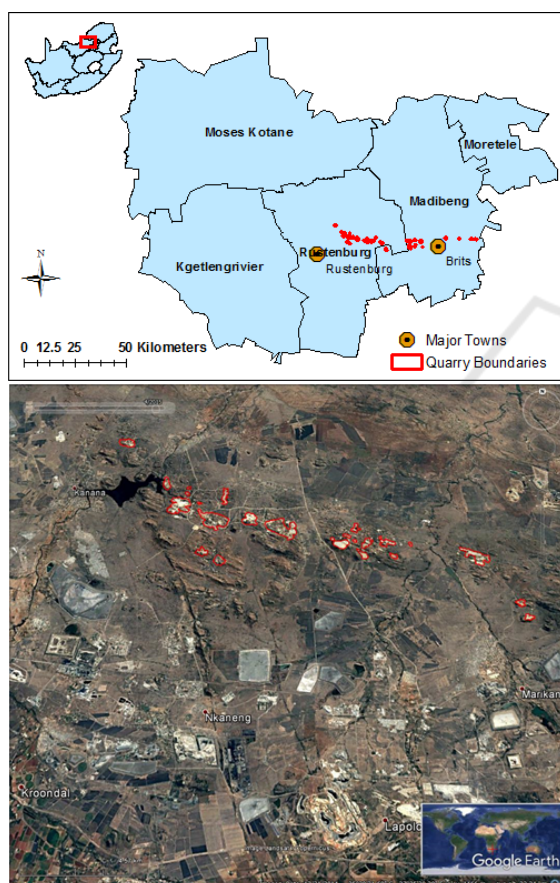


Figure 1: Maps showing (Top): Location of the study area and granite quarries (Bottom): Landscape of quarries and surrounding area.

### 3 METHODOLOGY

A minimum spatial coverage of 1 hectare and 200 m distance between the quarries were specified for quarry samples. The specification were set out to avoid overlap of samples, to promote independent comparison of quarries and to enhance detection with spatial resolution of remote sensing data. As a result, forty granite quarries were sampled for the study.

Since the launch of Google Earth™ in 2005, people have been using it to explore the world around them (Cha and Park, 2007). It provides images with high spatial resolution (<2.5 m) that are useful for land use and land cover mapping (Hu *et al.*, 2013). Sampling was achieved using geographical coordinates of known quarries. The coordinates were overlain on Google Earth™ to digitize the quarries and subsequently convert the polygons to shapefiles in ArcGIS® (ESRI 2016, ArcMap 10.4, Redlands, California, USA). Digitization process was done with the corresponding dates of acquired remote sensing data and therefore, the year 2015 and 2013 were used to digitize the quarries on Google Earth™. Quarries corresponding to remote sensing data acquired in earlier years before 2005 could not be used for digitization due to lack of data in Google Earth™.

#### 3.1 Remote Sensing Data

Data used in this study included Landsat images acquired on the 16<sup>th</sup> March 1998 and 16<sup>th</sup> April 2015 while ASTER data was acquired on the 26<sup>th</sup> April 2001 and 11 October 2013. The data was acquired from the United States Geological Survey (<https://earthexplorer.usgs.gov/>). Attempts were made to acquire images of same or close dates for consistent comparison between Landsat and ASTER data however, most of ASTER data was covered with clouds and therefore only available cloud free data was considered. The study preferred the use of data acquired during high rainfall summer season when vegetation is denser, however, unavailability of suitable data necessitated the use of images outside of this time period.

#### 3.2 Data Processing

##### 3.2.1 Image Registration of ASTER Data

Image registration process involves matching two or more images which were taken from different sensors at different times (Wahed *et al.*, 2013). Accuracy in image registration is important as this can significantly affect the results of change detection process. As a result, image registration accuracy should be limited to half or one pixel in change detection (Townshend *et al.*, 1992). In this study, the acquired ASTER data was firstly converted from hierarchical data format (HDF) file to tagged image file format (TIFF) file in ERDAS IMAGINE software (ERDAS IMAGINE® 2016, Hexagon Geospatial, Norcross, USA). After converting ASTER data from hdf to tiff format, image registration was performed

using automated registration technique in ArcGIS® 10.4 on the 2001 and 2013 ASTER images using Landsat 1998 and 2015 images as reference data. Registration accuracy for both 2001 and 2013 images were within one pixel in each dataset.

### 3.2.2 Radiometric Calibration

Radiometric calibration is an important step required to improve quality of remotely sensed data by removing factors that alters spectral properties of land surface features (Pons *et al.*, 2014). Both Landsat and ASTER images were radiometrically calibrated using absolute calibration method. This enables comparison of images acquired at different times from different sensors (Chander *et al.*, 2009). Data was calibrated by firstly converting the digital numbers (DNs) to at-sensor spectral. The second step involved converting at-sensor spectral radiance to exoatmospheric top of atmosphere (TOA) reflectance (Chander *et al.*, 2009). Equations applicable Landsat data are explained by (Chander *et al.*, 2009) while those applicable for ASTER data are provided by (Abrams and Hook, 2002).

### 3.2.3 Supervised Classification

Supervised classification was applied to multispectral images created from Landsat and ASTER data. The technique requires the user to select training samples which are representative of the desired classes to be identified. The quality of this classification method depends highly on the quality of training classes (Perumal and Bhaskaran, 2010). Supervised classification involves three principle steps. The first step involves defining training classes, the second step is creation of signature file and the last step is classification of the image (Lillesand *et al.*, 2014). Maximum likelihood classifier (MLC) algorithm was used to classify multispectral images. This method uses the training data by means of estimating means and variances of the classes, which are used to estimate probabilities and also consider the variability of brightness values in each class (Perumal and Bhaskaran, 2010). The effectiveness of MLC depends highly on accuracy of training samples (Richards, 2012).

### 3.2.4 Accuracy Assessment

Accuracy assessment was carried out on the Landsat 2015 and ASTER 2013 classified images. Error matrix was used to evaluate the accuracy of classification. A random set of 189 points were selected for error matrix. These points were overlain

on Google Earth™; the name of each class was then recorded using visual interpretation of land cover features on Google Earth™. The recorded class names in the reference data were then compared to classes generated from each image and the supervised classification. Google Earth™ has been used in a number of studies as a source of reference against which classification could be compared (Cha and Park, 2007; Rwanga and Ndambuki, 2017). Error matrix was generated and accuracy assessment parameters i.e. producer's accuracy (measure of omission errors), user's accuracy (measure of commission errors) and Kappa coefficient (measure of agreement) were computed.

### 3.2.5 Change Detection

Change detection involves four major aspects: (1) detecting that changes have occurred, (2) identify-ing the nature of the change, (3) measuring the areal extend of the change and (4) assessing the spatial pattern of the change (Congalton and Green, 2008). Various techniques used to perform change detection with digital imagery has been described by Singh (1989). This study utilized post-classification and Normalized Difference Vegetation Index (NDVI) change detection techniques to assess land cover changes within granite quarries. In post- classification comparison, each image is classified independently and then classification results are compared to determine areas and magnitude of change (Singh, 1989). The NDVI has been widely used to measure vegetation condition and biomass (Jiang *et al.*, 2006). It is defined as the difference between the near-infrared band (NIR) and the red band divided by the sum of these two bands (Tucker, 1979). The results of NDVI range between -1 and +1, where negative values correspond to absence of vegetation and positive values correspond to vegetated zones. The higher the index, the greater the chlorophyll content of the target (Pettorelli, 2013).

## 4 RESULTS

### 4.1 Accuracy Assessment

Error matrix for Landsat image is presented in Table 1. Overall accuracy obtained for Landsat data was 75% with Kappa coefficient of 0.71. Error matrix demonstrated that Water bodies had perfect producer's and user's accuracy. Granite quarries had moderate producer's accuracy due to confusion with Exposed rock formation, Bare land, Built-up land and Other

mining areas. Results for user’s accuracy however, were very high with limited confusion from Other mining areas. Results of other classes showed misclassification with other classes i.e.: Bare land and Vegetation had good producer’s accuracies but were also confused with each other. Other mining areas were confused with Bare land, Built-up land and Granite quarries. Exposed rock formation resulted in low producer’s accuracy due to confusion with Bare land and Built-up land. Similarly, Built-up land was confused with Bare land and that resulted in low producer’s accuracy of Built-up land.

Overall accuracy obtained for ASTER imagery was 79% with kappa coefficient of 0.75 (Table 2). Similar to Landsat classification, there was also confusion in classification of features. Water bodies had perfect producer’s and user’s accuracy. Producer’s accuracy for Granite quarries was high, however, was confused with Vegetation. Misclassi-

fication of Exposed rock formation was observed due to Granite quarries, Bare land, Built-up land and Vegetation. Relatively low producer’s accuracy was obtained for Other mining areas, due to mostly confusion with Granite quarries, Built-up land, Bare land and Vegetation. On the contrary, user’s accuracy for Other mining areas was perfect. Similarly, Exposed rock formation had almost perfect user’s accuracy with limited confusion observed with Bare land. Granite quarries had high user’s accuracy, but were confused with Exposed mining areas, Vegetation, and Other mining areas. Low user’s accuracy in Bare land was caused by misclassification from Other mining area, Built-up land, Exposed rock formation and Vegetation. Similarly, low user’s accuracy in Vegetation was a result of confusion caused by Granite quarries, built-up land, Bare land, Other mining areas and Exposed rock formation.

Table 1: Error matrix of classification derived from Landsat imagery in 2015.

		Reference Data								
		WB	GQ	ER	BUL	BL	V	OMA	Tot.	UA (%)
Classified Data	WB	10	0	0	0	0	0	0	10	100
	GQ	0	20	0	0	0	0	1	21	95
	ER	0	3	19	0	0	0	0	22	86
	BUL	0	2	2	19	0	0	3	26	73
	BL	0	1	9	11	24	3	4	52	46
	V	0	0	0	0	6	27	0	33	82
	OMA	0	3	0	0	0	0	22	25	88
	Tot.	10	29	30	30	30	30	30	141	
	PA (%)	100	69	63	63	80	90	73		
	Overall accuracy = 75%, Kappa = 0.71									

Key: WB=Water Bodies, GQ= Granite Quarries, ER= Exposed Rock Formations, BUL=Built-Up Land, BL=Bara Land, V=Vegetation, OM= Other Mining Areas, Tot. =Total, PA=Producer’s Accuracy, UA= User’s Accuracy.

Table 2: Error matrix derived from ASTER imagery taken in 2013 (Key definitions similar as in Table 2).

		Reference Data								
		WB	GQ	ER	BUL	BL	V	OMA	Tot.	UA (%)
Classified Data	WB	10	0	0	0	0	0	0	10	100
	GQ	0	26	1	0	0	1	1	29	90
	ER	0	0	24	0	1	0	0	25	96
	BUL	0	0	1	21	0	1	3	26	81
	BL	0	0	2	6	24	4	3	39	62
	V	0	3	2	3	4	26	4	42	62
	OMA	0	0	0	0	0	0	19	19	100
	Tot.	10	29	30	30	29	32	30	150	
	PA (%)	100	90	80	70	83	81	63		
	Overall accuracy = 79%, Kappa = 0.75									

## 4.2 Post-classification Change Detection

Figure 2 shows an example of land cover change within granite quarry boundaries on a zoomed portion of the study area. Seven land cover types generated from Landsat and ASTER classification analysis included (1) Water bodies, (2) Vegetation (3) Other mining areas (4) Granite quarries, (5) exposed rock formation, (6) Built-up land and (7) Bare land. The results from Landsat data classification in the whole study area revealed that dominant land cover types in 1998 were Vegetation, Bare land, natural Water bodies and Exposed rock formation with moderate occurrences of Granite quarries. In the year 2015 there was an increase in Granite quarries, Built-up land as well as Water bodies inside the quarries. A decrease in Vegetation and Bare land was observed in the year 2015. Figure 2 shows portions of the study area where development of granite quarries evolved (2015) on the land that did not have quarries before (1998).

Results of classification of ASTER images

revealed that Granite quarries were lesser in 2001 compared to the year 2013. Land cover in 2001 was dominated by Vegetation and Bare land, natural Water bodies, Exposed rock formation and to a lesser extent, covered with granite quarries. Classification of 2013 image however, revealed an increase in Granite quarries relative to those detected in 2001 as well as an increase in water bodies inside the quarries. The 2013 image also revealed loss in Bare land and increase in Exposed rock formation. Similarly, Figure 2 shows a portion of land cover that did not have granite quarries in 2001 but evolved in the year 2013.

### 4.2.1 Quantitative Measures of Land Cover change

The measure of areal extent of land cover change based on forty quarries between 1998 and 2015 for Landsat is given in Table 3. The results reveal significant increase in Granite quarries which subsequently resulted in accumulation of Water bodies. Increase in Granite quarries also resulted in significant loss of Vegetation and Bare land.

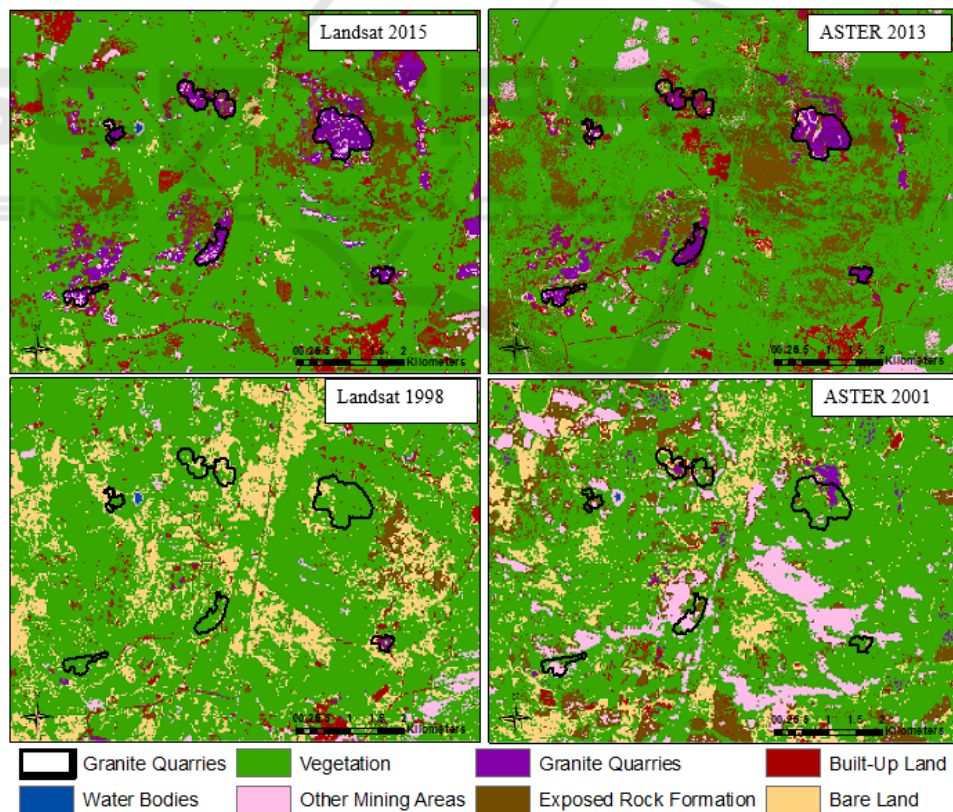


Figure 2: Land cover distributions created using supervised classification. Left images: land cover change within granite quarries derived from Landsat imagery (1998 and 2015). Right images: land cover change within granite quarries derived from ASTER imagery (2001 and 2013).

Table 3: Measure of land cover change within granite quarries based on Landsat classification data.

Classes	Area of classes (ha)		Difference (ha)
	1998	2015	2015-1998
Water Bodies	0.2	2.07	1.9
Granite Quarries	433.5	910.4	476.9
Bare Land	19.2	2.7	-16.5
Vegetation	793.7	313.1	-480.6

Similarly, the measure of change within granite quarries using ASTER data revealed more or less the same as those obtained from Landsat data.

Table 4 presents quantitative measure of land cover change based on ASTER data.

Table 4: Measure of land cover change using ASTER data.

Classes	Area of classes (ha)		Difference (ha)
	2001	2013	2013-2001
Water Bodies	0.2	2.4	2.23
Granite Quarries	213.1	745.1	531.9
Bare Land	219.5	157.4	-62.1
Vegetation	704.2	236.5	-467.7

Increase in Water bodies as detected by ASTER is more relative to results obtained from Landsat. There was a significant increase in Granite quarries while Vegetation and Bare land decreased significantly.

### 4.3 Change Detection using NDVI

Comparison of mean NDVI values within granite quarries using Landsat and ASTER data is presented in Figure 3. High mean NDVI values are observed in the year 1998 indicating more presence of green vegetation than in 2015. Mean NDVI values within quarries in 1998 range from 0.17 to 0.54 while for quarries in 2015 the range is between 0.05–0.3. Majority of quarries in 2001 have mean NDVI values above 0.25 while in 2013 majority have mean NDVI values below 0.1. Quarry 27 shows lowest mean NDVI value in the year 2001 whereas in 2013 and 2015, the quarry shows high mean NDVI values. This is a typical example of an abandoned quarry where revegetation is taking place. One quarry (Quarry #1) was sampled to evaluate NDVI pattern based on individual pixels within the quarry. NDVI histogram of Landsat data based on 322 pixels revealed that 79% of pixels in the year 1998 have NDVI values above 0.29. On the contrary, 45% of pixels in the year 2015 have NDVI values equal or less than 0.148 while other pixels show distribution across a range of NDVI values.

Analysis of NDVI values using ASTER data was based on 1296 pixels in the same quarry. Results showed that 100% of the pixels in the year 2013 have NDVI values between 0 and 0.233 while majority of pixels in the year 2001 are distributed above 0.233 NDVI values.

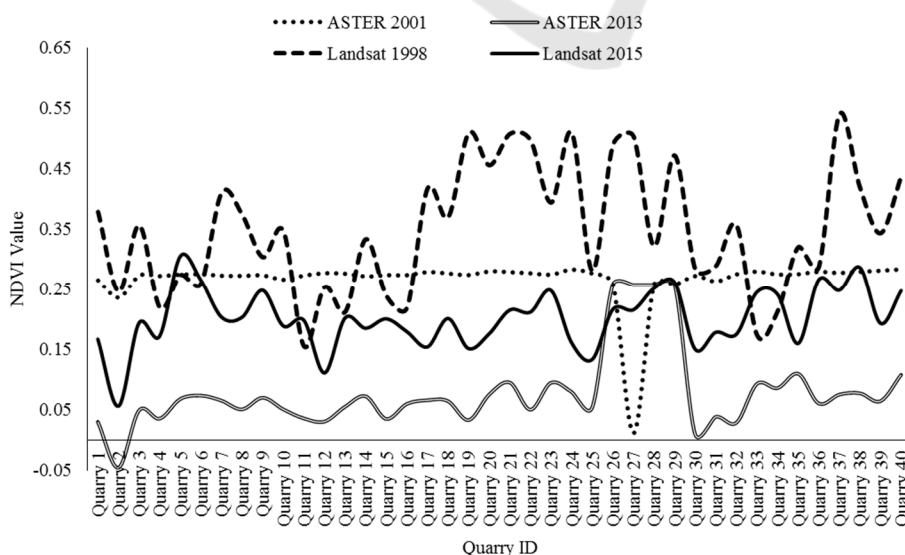


Figure 3: Comparison of mean NDVI values within granite quarries using Landsat and ASTER data.

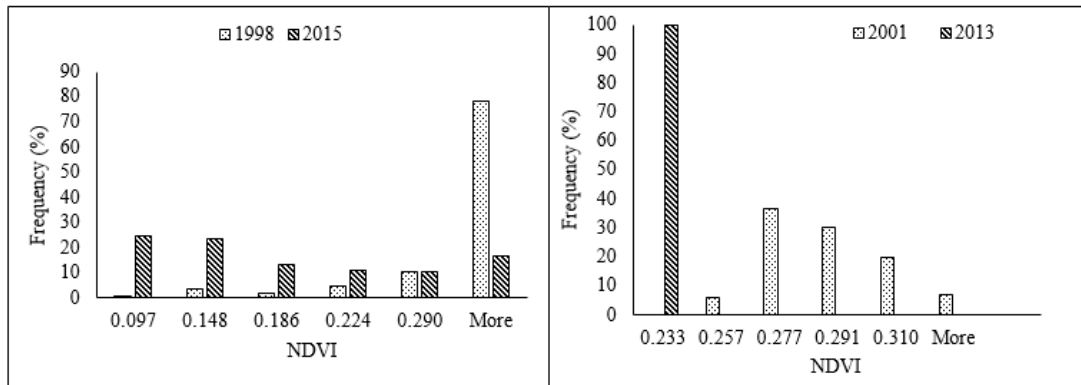


Figure 4: NDVI frequency distribution graphs for (left) Landsat data using 322 pixels at 30 m spatial resolution and (right) ASTER data using 1296 pixels at 15 m spatial resolution.

## 5 DISCUSSIONS

The aim of this study was to compare utility of Landsat and ASTER in land cover change detection within granite quarries. Both Landsat and ASTER proved effective in mapping and detecting land cover changes within granite quarries. Misclassification of classes was encountered in both classification of Landsat and ASTER imagery. Land cover change detection using both satellite sensors revealed a significant increase in Granite quarries. This increase subsequently resulted in loss of Vegetation and Bare land. Expansion of Granite quarries also resulted in accumulation of Water bodies inside the quarries. Mouflis *et al.* (2008) and Koruyan *et al.* (2012) have also demonstrated capabilities of Landsat and ASTER in monitoring land cover changes caused by expansion in marble quarries.

NDVI change detection analysis revealed decrease in green Vegetation cover within the acquired data period for both Landsat and ASTER. Results of NDVI derived from Landsat indicated that mean NDVI comparison between 1998 and 2015 varies across all quarry samples. Results obtained from ASTER data, showed that majority of quarries (95%) in 2001 displayed mean NDVI values between 0.25-0.3 while for 2013, majority (90%) of quarries had mean NDVI values below 0.1. Decrease in green Vegetation within granite quarries indicates the proliferation of quarrying activity over the acquired data periods. On the contrary, an increase in Vegetation on other quarries indicates revegetation process in abandoned quarries.

Although Landsat and ASTER were able to map land cover changes within granite quarries. ASTER data was found to be more effective in discriminating

Granite quarries and small Water bodies within granite quarries. This is attributed to the higher spatial resolution of ASTER in the visible and near infrared of electromagnetic spectrum than Landsat's (15 m vs 30 m). On the other hand, analysis of NDVI change detection revealed that Landsat sensor was better at detecting green Vegetation compared to results obtained using ASTER data.

Similar observations were recorded by Chevrel *et al.* (2005) who demonstrated capabilities of ASTER data in identifying and mapping surface disturbances due to mining. Charou *et al.* (2010), also demonstrated the effectiveness of ASTER in monitoring anomalies of water surfaces compared to Landsat and SPOT. Similarly, Musa and Jiya (2011) demonstrated the effectiveness of Landsat in assessing mining activities impacts on vegetation using NDVI.

## 6 CONCLUSION

Comparison of Landsat and ASTER data in change detection within granite quarries was evaluated in this study. Overall accuracy of classification using supervised classification and MLC for Landsat was 75% with kappa coefficient of 0.71, while ASTER returned a slightly better overall classification accuracy (79%) and kappa coefficient (0.75). Land cover mapping using Landsat data had limitation in detecting water bodies within granite quarries due to inadequate spatial resolution of the image relative to water body sizes. Vegetation cover was well discriminated in Landsat as compared to ASTER data. ASTER was found more effective in delineating granite quarries as compared to Landsat and this is attributed to the high spatial resolution of ASTER in

the visible and near infrared of the electromagnetic spectrum.

## REFERENCES

- Abrams, M. and Hook, S. (2002) 'ASTER User Hand-book Version 2', *Jet Propulsion*, 4800, pp. 1–135.
- Cha, S. and Park, C. (2007) 'The utilization of google earth images as reference data for the multitemporal land cover classification with MODIS data of north Korea', *Korean Journal of Remote Sensing*, pp. 483–491.
- Chander, G., Markham, B. L. and Helder, D. L. (2009) 'Summary of current radiometric calibration coefficients for Landsat MSS, TM, ETM+, and EO-1 ALI sensors', *Remote Sensing of Environment*. Elsevier Inc., 113(5), pp. 893–903.
- Charou, E., Stefouli, M., Dimitrakopoulos, D., Vasiliou, E. and Mavrantza, O. D. (2010) 'Using remote sensing to assess impact of mining activities on land and water resources', *Mine Water and the Environment*, 29(1), pp. 45–52.
- Chevrel, S., Bourguignon, A., Cottard, F. and Itard, Y. (2005) 'Exploitation of ASTER imagery in mining-related environmental management', in *Pecora 16 - Global Priorities in Land Remote Sensing*. Sioux Falls, South Dakota, pp. 1–10.
- Congalton, R. G. and Green, K. (2008) *Assessing the Accuracy of Remotely Sensed Data: Principles and Practices*. Second Edi. Boca Raton: CRC Press.
- Darwish, T., Khater, C., Jomaa, I., Stehouwer, R., Shaban, A. and Hamze, M. (2011) 'Environmental impact of quarries on natural resources in Lebanon', *Land and degradation and Development*, 22, pp. 345–358.
- Demirel, N., Emil, M. K. and Duzgun, H. S. (2011) 'Surface coal mine area monitoring using multi-temporal high-resolution satellite imagery', *International Journal of Coal Geology*. Elsevier B.V., 86(1), pp. 3–11.
- Dolley, T. P. (2007) 'Stone, Dimension'. USGS Minerals Yearbook, 1, pp. 1–11.
- Hu, Q., Wu, W., Xia, T., Yu, Q., Yang, P., Li, Z. and Song, Q. (2013) 'Exploring the use of google earth imagery and object-based methods in land use/cover mapping', *Remote Sensing*, 5(11), pp. 6026–6042.
- Jiang, Z., Huete, A. R., Chen, J., Chen, Y., Li, J., Yan, G. and Zhang, X. (2006) 'Analysis of NDVI and scaled difference vegetation index retrievals of vegetation fraction', *Remote Sensing of Environment*, 101(3), pp. 366–378. doi: 10.1016/j.rse.2006.01.003.
- Koruyan, K., Deliormanli, a. H., Karaca, Z., Momayez, M., Lu, H. and Yalçın, E. (2012) 'Remote sensing in management of mining land and proximate habitat', *Journal of the Southern African Institute of Mining and Metallurgy*, 112(7), pp. 667–672.
- Lamprecht, A. J. H., Cilliers, S. S., Götze, A. R. and Du Toit, M. J. (2011) 'Phytosociological description of norite koppies in the Rustenburg area, North-West Province and refinement of the distribution of the Norite Koppies Bushveld on the national vegetation classification map of South Africa', *Bothalia*, 41(2), pp. 327–339.
- Latifovic, R. (2005) *Satellite RemoteSensing in Assessing the Environmental Impactsof Large-Scale Surface Mining*. PhD Thesis, Department De Genie Des Mines, De La Metallurgie Et Des, Univerite Laval Quebec.
- Lillesand, T., Kiefer, R. W. and Chipman, J. (2014) *Remote Sensing and Image Interpretation*. 7th edn. New York: John Wiley & Sons.
- López-Pamo, E., Baretino, D., Antón-Pacheco, C., Ortiz, G., Arránz, J. C., Gumiel, J. C., Martínez-Pledel, B., Aparicio, M. and Montouto, O. (1999) 'The extent of the Aznalcollar pyritic sludge spill and its effects on soils', *Science of the Total Environment*, 242(1–3), pp. 57–88.
- Lu, D., Mausel, P., Brondizio, E. and Moran, E. F. (2004) 'Change detection techniques', *International Journal of Remote Sensing*, 25(February), pp. 2365–2407.
- Maponga, O. and Munyanduri, N. (2001) 'Sustainability of the dimension stone industry in Zimbabwe—challenges and opportunities', *Natural Resources Forum*, 25(3), pp. 203–213.
- Mouflis, G. D., Gitas, I. Z., Iliadou, S. and Mitri, G. H. (2008) 'Assessment of the visual impact of marble quarry expansion (1984-2000) on the landscape of Thasos island, NE Greece', *Landscape and Urban Planning*, 86(1), pp. 92–102.
- Musa, H. D. and Jiya, S. N. (2011) 'An Assessment of Mining Activities Impact on Vegetation in Bukuru Jos Plateau State Nigeria Using Normalized Differential Vegetation Index (NDVI)', *Journal of Sustainable Development*, 4(6), pp. 150–159.
- Nex, P. A., Kinnaird, J. A., Ingle, L. J., Van Der vyver, B. A. and Cawthorn, R. G. (1998) 'A new stratigraphy for the main zone of the Bushveld Complex, in the Rustenburg area', *South African Journal of Geology*, 101(3), pp. 215–223.
- Paull, D., Banks, G., Ballard, C. and Gillieson, D. (2006) 'Monitoring the Environmental Impact of Mining in Remote Locations through Remotely Sensed Data', *Geocarto International*, 21(1), pp. 33–42.
- Perumal, K. and Bhaskaran, R. (2010) 'Supervised classification performance of multispectral images', *Journal of Computing*, 2(2), pp. 124–129.
- Pettorelli, N. (2013) *The Normalized Difference Vegetation Index*. New York, USA: OUP Oxford.
- Pons, X., Pesquer, L., Cristóbal, J. and González-Guerrero, O. (2014) 'Automatic and improved radiometric correction of landsat imageryusing reference values from MODIS surface reflectance images', *International Journal of Applied Earth Observation and Geoinformation*. Elsevier B.V., 33(1), pp. 243–254.
- Richards, J. A. (2012) *Remote Sensing Digital Image Analysis: An Introduction*. Berlin Heidelberg: Springer Science & Business Media.
- Rogan, J. and Chen, D. (2004) 'Remote sensing technology for mapping and monitoring land-cover and land-use change', *Progress in Planning*, 61, pp. 301–325.

- Rwanga, S. S. and Ndambuki, J. M. (2017) 'Accuracy Assessment of Land Use/Land Cover Classification Using Remote Sensing and GIS', *International Journal of Geosciences*, 8(4), pp. 611–622.
- Singh, A. (1989) 'Review Article Digital change detection techniques using remotely-sensed data', *International Journal of Remote Sensing*, 10(6), pp. 989–1003.
- Townshend, J. R. G., Gurney, C., McManus, J. and Justice, C. O. (1992) 'The Impact of Misregistration on Change Detection', *IEEE Transactions on Geoscience and Remote Sensing*, 30(5), pp. 1054–1060.
- Tucker, C. J. (1979) 'Red and photographic infrared linear combinations for monitoring vegetation', *Remote Sensing of Environment*, 8(2), pp. 127–150.
- Wahed, M., El-tawel, G. S. and Gad El-karim, A. (2013) 'Automatic Image Registration Technique of Remote Sensing Images', *International Journal of Advanced Computer Science & Applications*, 4(2), pp. 177–187.

